Journal of Materials Chemistry A

Accepted Manuscript

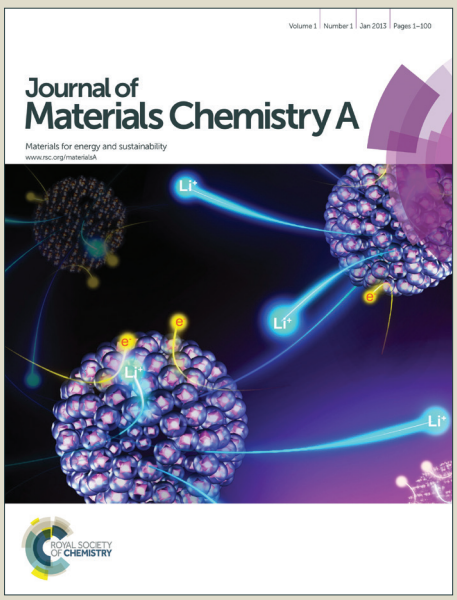

ROYAL SOCIETY OF CHEMISTRY

www.rsc.org/materialsA

Crosslinked Polyaniline Nanorods with Improved Electrochemical Performance as Electrode Material for Supercapacitor

*Xue Wang, Jinxing Deng, Xiaojuan Duan, Dong Liu, Jinshan Guo and Peng Liu**

State Key Laboratory of Applied Organic Chemistry and Resources Utilization of Gansu Province, College of Chemistry and Chemical Engineering, Lanzhou University, Lanzhou 730000, China

AUTHOR INFORMATION

Corresponding Author

*E-mail: pliu@lzu.edu.cn. Tel./Fax: 86-931-8912582.

Abstract

In order to improve the electrochemical performance of polyaniline (PANI), the crosslinked polyaniline nanorods (CPANI) were prepared via chemical oxidative copolymerization of aniline with *p*-phenylenediamine (PPDA) and triphenylamine (TPA). Their morphology and structure were compared with polyaniline (PANI) via Transmission electron microscopy (TEM), Scanning electron microscopy (SEM), Fourier transform infrared spectroscopy (FTIR), X-ray powder diffraction (XRD) and Thermogravimetric analysis (TGA) techniques. The CPANI nanorods exhibited an improved electrical conductivity (33.3 S cm^{-1}) in comparison with the PANI (4.26 S cm^{-1}). Its electrochemical performance was studied by galvanostatic charge/discharge (GCD), cyclic voltommetry (CV) and electrochemical impedance spectroscopy (EIS) tests. The CPANI nanorods exhibited a maximum specific capacitance of 455.1 F g^{-1} at a scan rate of 1 mV s^{-1} in 1.0 mol L^{-1} H_2SO_4 electrolyte, also much higher than that of the PANI (286.7 F g^{-1}). Notably, the cycling stability of the CPANI electrode had been improved significantly by the chemical crosslinking, and could remain higher capacitance retention after 1300 cycles.

Keywords: Polyaniline; Crosslinked; Nanorods; *In-situ* copolymerization; Electrochemical performance

1. INTRODUCTION

At present, the electrochemical supercapacitors, as energy storage devices between secondary batteries and traditional capacitors, has been considerably focused due to their remarkable properties including high capacitance, high power density, wide thermal operating range, and environmental friendliness.[1] Carbon materials, metal oxides and conducting polymers are commonly taken for potential electrode materials for electrochemical supercapacitors. Actually, the transition metal oxides display high specific capacitance. However, the high cost and toxicity limit their application.[2] Carbon materials exhibit long cycle life, but low specific capacitance.[3] These disadvantages hinder their practical applications for electrode materials of supercapacitors.

In contrast, the nanostructured conducting polymers, such as polyaniline (PANI), polypyrrole (PPy) and polythiophene (PTh), have been regarded as promising electrode materials for supercapacitors. Among these conducting polymers, PANI is famous for its morphology diversity (nanofibers, nanotubes and nanowires etc), high electrical conductivity, large specific surface, good redox reversibility, low cost, and simple synthesis.[4] Regrettably, as an electrode material for supercapacitors, PANI exhibits poor cycling stability due to the volume change during the long charge/discharge process.[5-7]

So far, many researchers have focused on the synthesis of inorganic/PANI hybrid materials in order to overcome its poor cycling stability, with the transition-metal oxides (such as MnO_2 and RuO_2)[8-10] or carbon materials (such as graphene[11-18] and carbon nanotubes[19-24]) as supporting materials. However, in the approach above-mentioned, each component in the hybrid materials still retains its own structure. And the improvement in cycling stability of PANI has been mainly

attributed to the contributions of these supporting materials or the synergistic effects between them in some cases.

Crosslinking might be a candidate to improve the electrical and electrochemical properties of the conductive polymers. Yang et al prepared the crosslinked PANI samples via the in-situ chemical oxidative polymerization of aniline in the presence of *p*-phenylenediamine (PPDA) and triphenylamine (TPA) with HCl as dopant.[25] The effect of the p-phenylenediamine and triphenylamine contents on the electrical conductivity of the crosslinked PANI was mainly discussed. By now, there is no report on the crosslinked PANI as electrode material for supercapacitors.

In the present work, the chemical crosslinking method is tried to improve the electrochemical properties of PANI by introducing the conjugated crosslinkers into the conjugated conducting polymer for the first time. To avoid the influence of the exchanging of dopant during the electrochemical process, H_2SO_4 was selected as the dopant in this work. The effects of the crosslinking reaction on the morphology, structure, and electrical conductivity of the CPANI were discussed in detail. And the electrochemical performance of the resulting copolymer was investigated in 1.0 mol L^{-1} H_2SO_4 aqueous solution.

2. EXPERIMENTAL METHODS

2.1. Materials

Analytical reagent grade aniline (An) and ammonium peroxodisulfate (APS) were purchased from Tianjin Guangfu Technology development Co. Ltd, Tianjin, China. Aniline was distilled under reduced pressure before use.

P-phenylenediamine (PPDA) and triphenylamine (TPA) were obtained from Tianjin Guangfu Fine Chemical Research Institute and Gracia Chemical Technology Co. Ltd, respectively. Ammonium persulfate (APS), N, N-dimethylformamide (DMF) and sulfuric acid (H_2SO_4) were used as received. Doubly deionized water was used through all the processes.

2.2. Synthesis of the crosslinked polyaniline and linear polyaniline

The crosslinked polyaniline (CPANI) was prepared as reported previously.[25] Typically, 0.01 mol of aniline was dissolved into a 100 mL 0.5 mol L^{-1} H_2SO_4 containing 0.0001 mol triphenylamine (TPA) and 0.0002 mol *p*-phenylenediamine (PPDA). Then, APS (2.2820 g (0.01 mol) in 20 mL 0.5 mol L^{-1} H_2SO_4) was added drop by drop into the solution, and the crosslinking polymerization was initiated and lasted for 10 h under stirring in an ice bath. For comparison, the homopolymer of aniline (PANI) was also synthesized by the similar procedure without PPDA and TPA.

2.3. Characterizations

The morphologies of the crosslinked and linear polymer samples (CPANI and PANI) were investigated with a JEM-1230 transmission electron microscopy (TEM) (JEOL, Tokyo, Japan) and a S-4800 scanning electron microscopy (SEM, Hitachi, Japan). For the TEM analysis, the samples were dispersed in water in an ultrasonic bath for 30 min, and dropped onto the Cu grids covered with a carbon film.

Fourier transform infrared (FT-IR) measurements (Impact 400, Nicolet, Waltham, MA) were recorded with the KBr pellet method in the wavelength range of 400-4000 cm^{-1}.

The ultraviolet-visible spectra (UV-vis) were obtained using a UV-vis spectrometer (TU-1901, Beijing Purkinje General Instrument, Co. Ltd, Beijing, China).

Elementary composition of the PANI and CPANI samples was conducted on an Elementar Vario EL instrument (Elementar Analysen systeme GmbH, Munich, Germany).

The crystal structures of samples were characterized using X-ray powder diffractometer (XRD, Panalytical X' Pert PRO X-ray Diffractometer). Nickel-filter Cu Kα radiation (λ = 0.15418 nm) was used with a generator voltage of 40 kV and a current of 30 mA.

Thermogravimetric analysis (TGA) data were performed on a thermal analysis instrument (Diamond TG thermogravimetric analyzer) with a heating rate of 10 °C min^{-1} in nitrogen atmosphere.

The electrical conductivities of the samples were recorded using a RTS-2 four-point probe conductivity tester ((Guangzhou four-point probe meter Electronic Technology Co., Ltd) at room temperature. The pellets were obtained by subjecting the powder samples to a pressure of 20 MPa. Each value given is an average of three times measurements.

All electrochemical experiments were carried out in a three-electrode system with a working electrode, a platinum counter electrode, and a standard calomel reference electrode (SCE). The working electrodes were fabricated with the mixture containing the active materials (the results copolymer), carbon black, and polyvinylidenefluoride (PVDF) with mass ratio of 80:15:5 to make homogeneous mixture in DMF. Galvanostatic charge-discharge tests (GCD), cyclic voltammetry (CV) and electrochemical impedance spectroscopy (EIS) of the samples were performed on a CHI660B electrochemical workstation in 1.0 M H_2SO_4 aqueous solution. The potential range for GCD and CV tests was -0.2 to 0.8 V. EIS tests were carried out ran at open circuit potential of 0.4 V in the frequency range from 100 kHz to 0.01 Hz with an AC perturbation of 5 mV.

3. RESULTS AND DISCUSSION

3.1. Morphology and structure

The CPANI nanorods were synthesized via the facile chemical oxidative polymerization of aniline with PPDA and TPA as the crosslinkers. Aniline and PPDA monomers are oxidized into cation radicals by APS. The polymerization of these phenylamino cation radicals produces linear poly(aniline-*p*-phenylenediamine) oligomers with two terminated amino groups. After oxidation, the linear poly(aniline-*p*-phenylenediamine) oligomer cation radicals continue to react with TPA to form the crosslinking network structure by simultaneous polymerization at three para-positions of N element due to the identical reaction activity (Scheme 1).

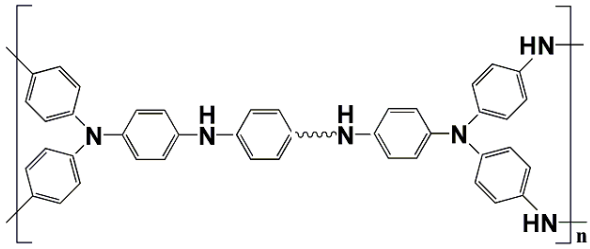

Scheme 1. Structure of the CPANI copolymer.

Their morphology was compared with the homopolymer of aniline (PANI) using TEM technique. The PANI sample shows a typical irregular morphology (Figure 1 a and b). As for the CPANI samples (Figure 1 c and d), more regular and ordered nanorods with diameters of about 50 nm and length of several hundred nm were observed from the higher magnification images (Figure 1 a and c, 100000 times). It indicated that the crosslinked polyaniline (CPANI) had been successfully prepared (Scheme 1), via the templating effect of PPDA and TPA due to their poor aqueous solubility.[25] As known, the well-aligned nanorod morphology with large surface area may be more beneficial to the electrical conductivity and specific capacitance than the normal PANI powder, when being used as electrode materials for supercapacitors.[26]

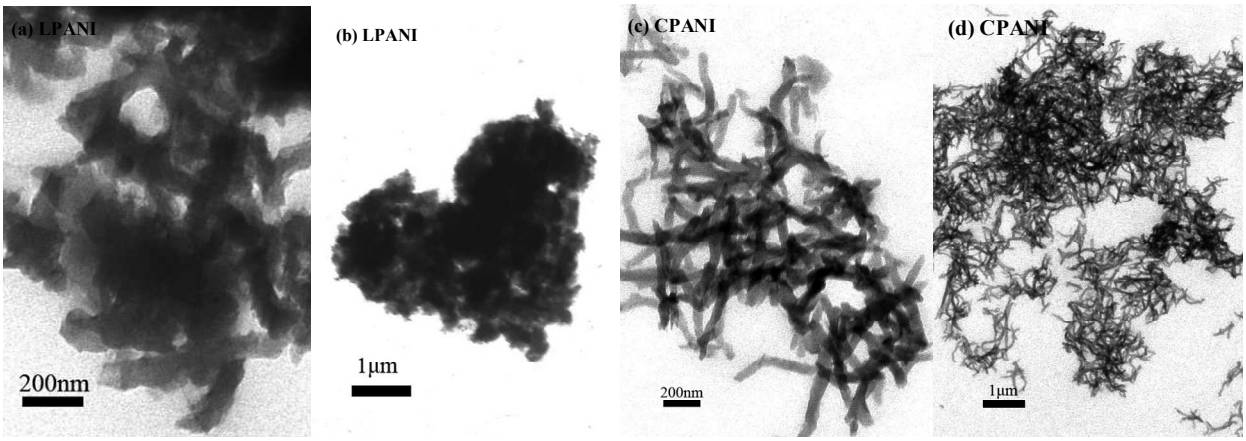

Figure 1. TEM images of the PANI (a, b) and CPANI (c, d) samples.

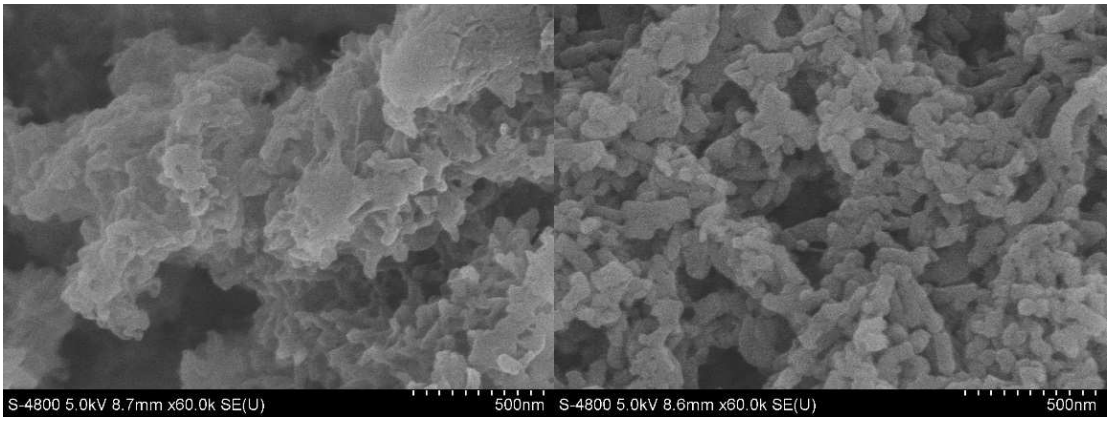

(a) PANI (b) CPANI

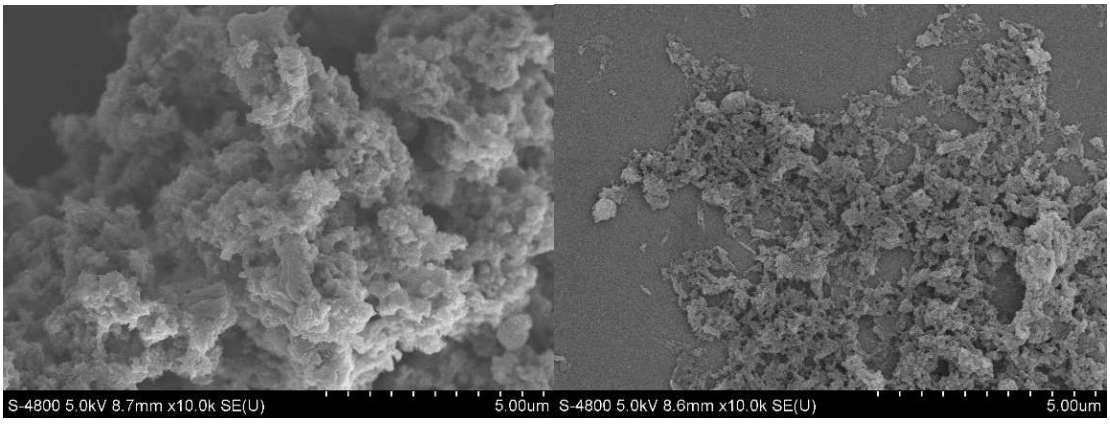

(c) PANI (d) CPANI

Figure 2. SEM images of the PANI and CPANI samples at high magnification (a and b) and low magnification (c and d).

The CPANI and PANI samples showed the similar characteristic absorbance peaks in the FT-IR spectra (Figure 3). The peaks at about 1580 and 1500 cm^{-1} are assigned to the C=C stretching mode of the quinonoid rings and benzenoid units. Two peaks at 1306 and 1241 cm^{-1} are attributed to the C-N stretching mode for the aromatic amine. The strongest peak at 1111 cm^{-1} is assigned to the vibration mode of $–NH^{+}=$, indicating the higher doping level.[27,28] The absorbance peak at around 800 cm^{-1} corresponding to the C-H out-of-plane bending vibration of the 1, 4-disubstituted rings can be seen in both the spectra.[29] However, for the CPANI nanorods, the peak intensity of the stretching vibration of the aromatic rings at 1645 cm^{-1} significantly increased, indicating an increase in the benzenoid content as a direct consequence of the copolymerization of PPDA and TPA.[25] The absorbance peak at 3450 cm^{-1} of the N-H stretching mode in the CPANI is much stronger than that of the PANI, attributing to the higher amine content in the CPANI due to the introduction of PPDA.

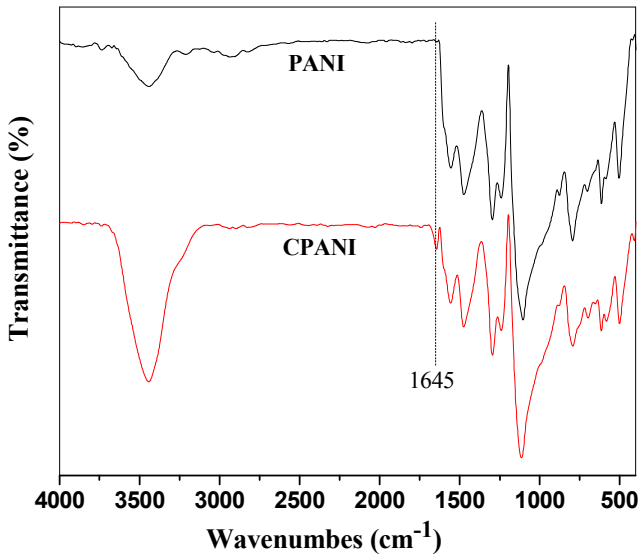

Figure 3. FT-IR spectra of the PANI and CPANI samples.

In order to further validate the structure of the CPANI, UV-Vis analysis was employed. The UV-Vis spectrum of the PANI is also presented to facilitate the comparative discussion. It can be observed from Figure 4a that the PANI and CPANI show the similar UV-vis absorption in ethanol. The peak at 350 nm is ascribed to the π-π* transition of the benzenoid rings and the peaks at 440 and 800 nm can be assigned to the polaron transition,[31,32] indicating that the samples are in the conductive emeraldine salt (ES) form in ethanol dispersion. Compare to the PANI, the CPANI exhibits higher intensity π-π* transition attributed to the introduction of the PPDA and TPA units. Moreover, this transition underwent a blue shift from 350 to 300 nm due to the electronic conjugation node introduced by TPA in the crosslinked network structure of the CPANI. [25,31]

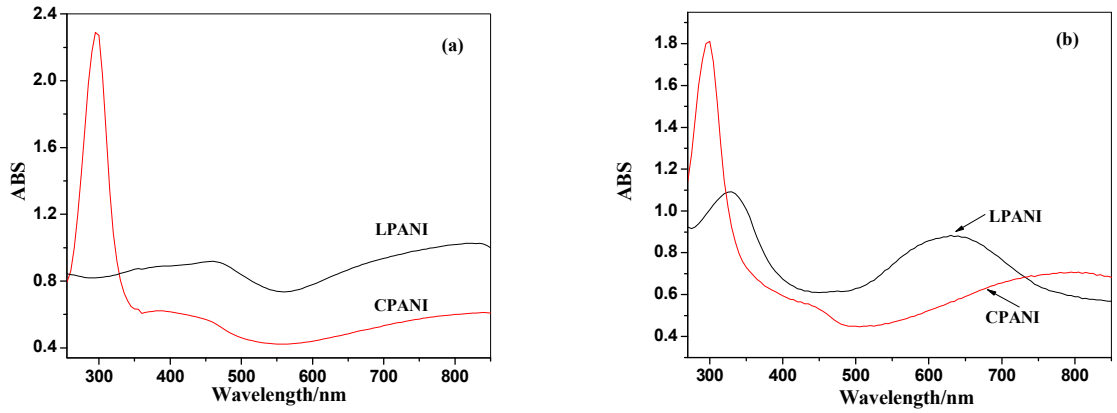

Figure 4. UV-vis spectra of the PANI and CPANI samples in ethanol (a) or DMF (b) dispersion.

By changing the solvent from ethanol to DMF (Figure 4b), it is clear that the polaron bands (440 and 800 nm) of the PANI disappeared, and the excitation of the quinoid rings appeared at 630 nm of the emeraldine base (EB) form,[33] as reported previously.[34-36] The results indicate that the doping level of the PANI decreases in DMF, which leads to its reduction from the ES to EB

form. In contrast, the UV-vis spectra of the CPANI are similar in both dispersions, implying that the CPANI can maintain more stable doped state than the PANI in aprotic solvent.

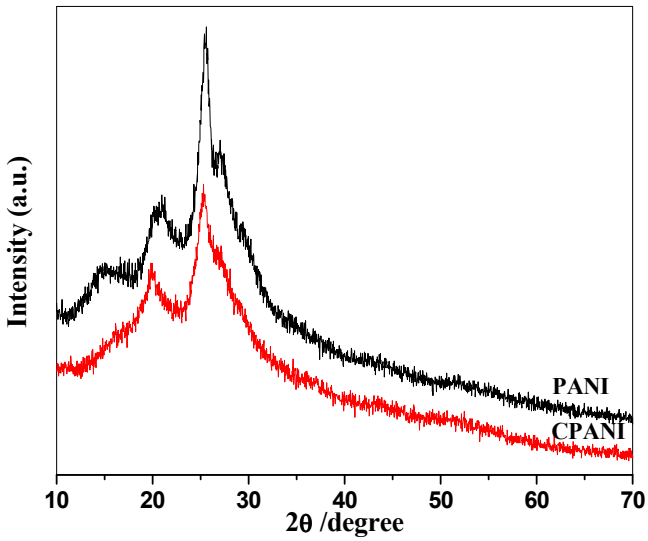

Figure 5. XRD patterns of the PANI and CPANI samples.

Figure 5 shows the typical X-ray powder diffraction patterns of the PANI and CPANI samples. For the PANI, the diffraction peaks at 2θ = 15.1°, 20.7° and 25.5° can be attributed to (011), (020) and (200) crystal planes of PANI in its ES form, respectively.[37] When the PPDA and TPA units were introduced, the diffraction peak at 15.1° and 25.5° of the CPANI nanorods decreased in relative intensity and became boarder. This result was attributed to the reduced degree of orientation and population of crystallites of the CPANI in (011) and (200) crystal planes due to that the PPDA and TPA units might hinder to the ordering of the polyaniline chains.[38,39] Although it was reported that PPDA had no effect on the crystallinity of PANI,[40] the addition of the TPA units twisted the polymer chains out of plane, led to the lower crystallinity of the copolymers.[41,42]

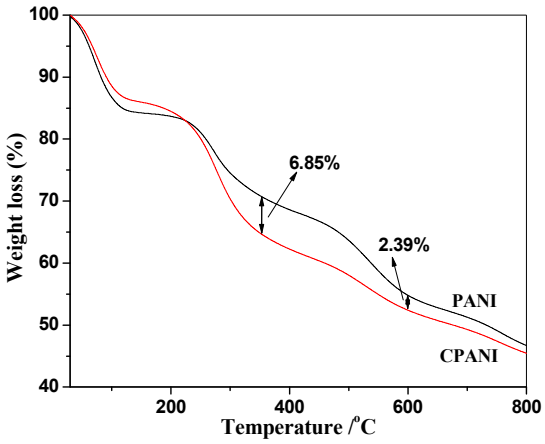

Figure 6. TGA curves of the PANI and CPANI samples.

The thermal stability of the PANI and CPANI samples has been investigated by TGA analysis under N_2 atmosphere (Figure 6). The initial weight loss in the range 30-120 ^{o}C is caused by the evaporation of moisture. From 120 to 350 ^{o}C, the weight loss of the PANI and CPANI samples is related to the removal of doping anions.[45] In this temperature range, the CPANI nanorods showed a higher mass loss (19.25 wt%) than that of the PANI (12.05 wt%) due to a higher doping level, which is consistent with elemental analysis result. In addition, the higher mass loss of the CPANI nanorods may be also attributed to the effect caused by the rapid degradation of poly(*p*-phenylenediamine)[44] via the homo-polymerization of *p*-phenylenediamine in the crosslinking copolymerization. The weight loss occurred in the temperature range of 350-600 ^{o}C corresponds to the decomposition of the polymer chains. From 350 to 600 ^{o}C, the weight losses were estimated to be 16.09wt% and 11.63wt% for the PANI and CPANI samples, respectively. The relatively slower weight loss of the CPANI sample than that of the PANI sample can be contributed to the hindering effect of crosslinked network structure on the decomposition of the CPANI nanorods (Scheme 1).

3.2. Electrical conductivity

The electrical conductivity of the PANI sample was measured to be 4.26 S cm^{-1} at room temperature. After the PPDA and TPA units were introduced, the electrical conductivity of the CPANI nanorods increased to 33.3 S cm^{-1}, due to the charge carriers delocalize in a large poly-conjugated network.[25] This result reflected the higher conjugated system and the higher extent of interchain interaction in the CPANI copolymers. This indicated that PPDA and TPA had a remarkable effect on the microstructure of the CPANI copolymer. In addition, the highly ordered structure of the CPANI copolymer may be favorable to a higher conductivity.

The different electrical conductivities could be revealed by element analysis. For the PANI, the C:N molar ratio was equal to the theoretical value (6.00:1). At the same time, its N:S molar ratio was calculated to be 3.34:1, implying that the partial doping state (about one third) of polyaniline led to the low electrical conductivity. In contrast, the N content (C:N=6.27:1) in the CPANI was much higher than the theoretical value (C:N=9.6:1). It implied that the linear poly(aniline-*p*-phenylenediamine) oligomers had been produced as the linkers between two crosslinking sites (TPA unit) during the chemical oxidative copolymerization. Furthermore, the high S content (N:S=1.28:1) in the CPANI demonstrated its high doping level. The high doping level of proton in CPANI composite can effectively reduce the barrier height, and the conjugated network provides a strong conjugated interaction for charge delocalization in intra-chain and inter-chain, so the CPANI nanorods exhibited the enhanced electrical conductivity.

3.3. Electrochemical performance

The electrochemical behavior of the CPANI nanorods was compared with the PANI using galvanostatic charging/discharging (GCD) and cyclic voltammetry (CV) techniques. The specific

capacitance (*Cm*) can be calculated according to $Cm=(\int IdV)/(mV\upsilon)$, where *Cm* is the specific capacitance, *I* is the response current density, *V* is the potential window, υ is the potential scan rate, and *m* is the mass of the active material in the working electrode.

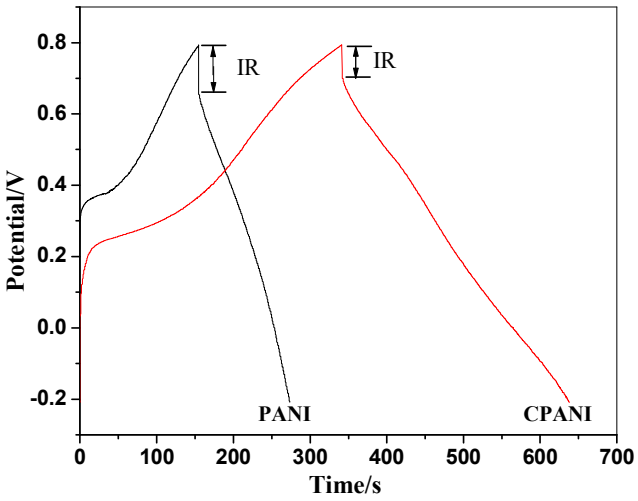

Figure 7. Galvanostatic charge/discharge curves of the PANI and CPANI electrodes in 1 mol L^{-1} H_2SO_4 at a current density of 1 A g^{-1}.

Figure 7 shows the galvanostatic charging/discharging (GCD) curves of the PANI and CPANI electrodes in 1 mol L^{-1} H_2SO_4 at a current density of 1 A g^{-1}. The curve of the CPANI electrode was not ideal symmetric profiles, exhibiting the following two voltage stages: the first voltage stage in the range of 0.8 to 0.6 V is ascribed to the electric double-layer (EDL) capacitance. In contrast, the second voltage stage in the range of 0.6 to -0.2 V with a longer discharge period implies that the electrode materials possess both EDL and Faradaic capacitances simultaneously.[13] The IR drop of the CPANI electrode caused by the internal resistance was lower than that of the PANI electrode, indicating that introducing PPDA and TPA units resulted in the improved capacitive behavior of the CPANI electrode. A higher specific capacitance of

297 F g^{-1} was achieved for the CPANI electrode in comparison with that of the PANI electrode (119 F g^{-1}) at a current density of 1 A g^{-1}. It means that the significant electrical double-layer capacitance and Faradic pseudocapacitance has been achieved due to its regular nanorod morphology with large surface area and the higher electrical conductivity.

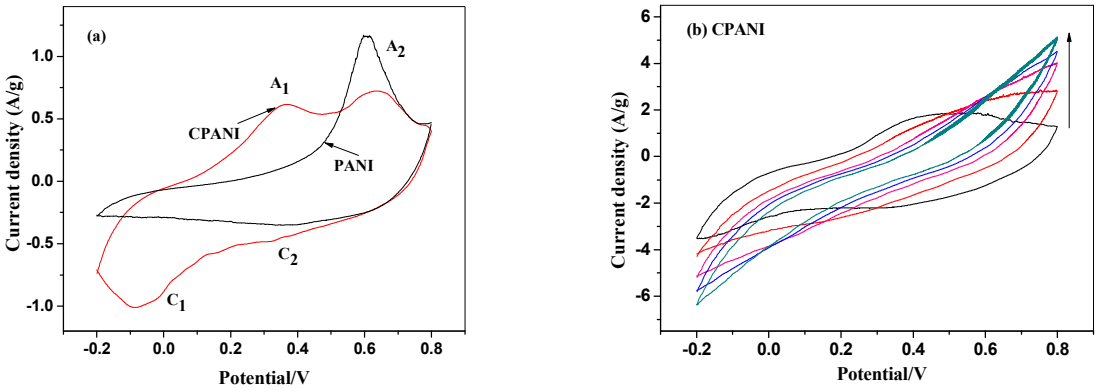

Figure 8. (a) Cyclic voltammetry curves of the PANI and CPANI electrodes at the scan rate of 1 mV s^{-1}, (b) Cyclic voltammetry curves of the CPANI electrode at different scan rates (5 mV s^{-1}, 10 mV s^{-1}, 20 mV s^{-1}, 30 mV s^{-1} and 50 mV s^{-1}).

Figure 8a shows the CV curves of the PANI and CPANI electrodes under a scan rate of 1 mV s^{-1} between -0.2 and 0.8 V (vs. SCE). Compared with the PANI electrode, the CPANI electrode displayed two pairs of redox peaks (A_1/C_1, A_2/C_2), attributed to the redox transitions of polyaniline: the leucoemeraldine-emeraldine (A_1/C_1) and emeraldine-pernigraniline (A_2/C_2) transformations, which results in the higher Faradaic capacitance.[43] While the CV curve of the PANI electrode showed a couple of the redox peaks (A_2/C_2) due to the transition between emeraldine-pernigraniline states. According to the CV curves, the specific capacitances of the CPANI and PANI electrodes were calculated to be 455.1 and 286.7 F g^{-1} at the scan rate of 1 mV s^{-1}, respectively.

The rate capability of the CPANI electrode was further evaluated by CV under various scan rates (5, 10, 20, 30 and 50 mV s^{-1}) (Figure 8b). Increasing the scan rate from 5 to 50 mV s^{-1}, the response current density gradually increased, demonstrating the good rate capability of the CPANI electrode. Moreover, the redox peaks of the CPANI electrode became less obvious with increasing the scan rate, mainly due to that the diffusion of the electrolyte ions is not so fast into the interior electrode. This indicates that the CPANI electrode mainly possesses the electrical double-layer capacitance at higher scan rate.

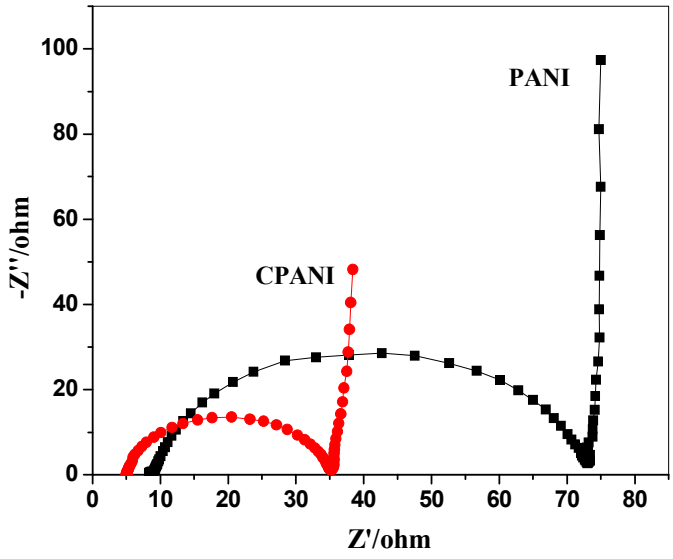

Figure 9. Nyquist plots of the PANI and CPANI electrodes.

The electrochemical performance of the PANI and CPANI electrodes was investigated by the electrochemical impedance spectrum (EIS) at an open circuit potential of 0.4 V. It can be observed from the typical Nyquist plots (Figure 9) that each impedance spectrum has two distinctive parts composing of a semicircular arc in the high frequency region and a straight line in the middle-to-low frequency region. The high-frequency arc represents the charge transfer resistance (R_{ct}) caused by the electrochemical reactions at the contact interface between electrode

and electrolyte solution.[46] The R_{ct} obtained from the semicircular arc diameter were 64.7 and 30.2 Ω for the PANI and CPANI electrodes, respectively. It is obvious that the R_{ct} of the CPANI electrode (30.2 Ω) is much lower than that of the PANI electrode (64.7 Ω). The straight line with a slope from 45° to 90° ascribes to the Warburg diffusion behavior. It can be observed that the CPANI electrode exhibits a short and vertical line, representative of fast ion diffusion/transport in the electrode material.[47] At the same time, the equivalent series resistance (R_s) can be observed from the X-intercept of Figure 9, which included the ionic resistance of electrolyte, intrinsic resistance of the active material, and contact resistance at the active material/current collector interface.[46,48] The PANI and CPANI electrodes delivered R_s of 8.32 and 4.96 Ω, respectively. The result of the Nyquist plots indicates that the CPANI electrode has an improved electrochemical capacitive behavior, which should be attributed to the higher conductivity and charge transfer capability of the crosslinked copolymer.

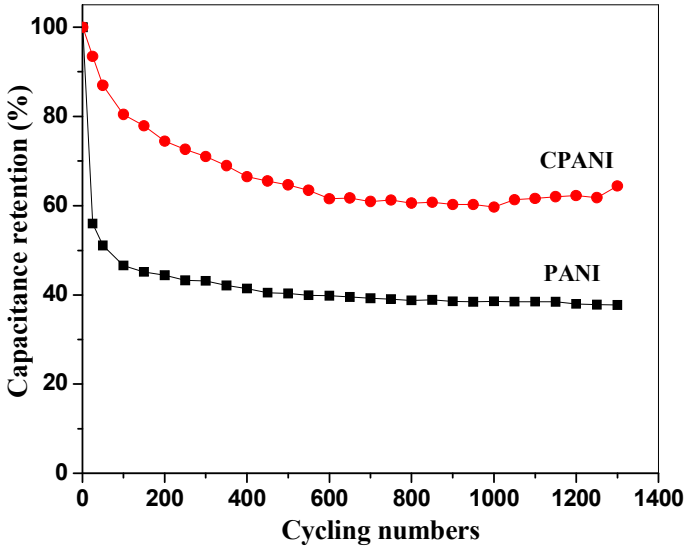

Figure 10. Cyclic stability of the PANI and CPANI electrodes at the scan rate of 100 mV s^{-1}.

The electrochemical stabilities of the PANI and CPANI electrodes was compared by CV cycling in 1.0 mol L^{-1} H_2SO_4 solution at 100 mV s^{-1} in the range of -0.2-0.8 V and the capacitance retentions are shown in Figure 10. It is observed that the specific capacitance of the PANI electrode decreased more rapidly (53% loss after 100 cycles) compared with the CPANI electrode. The higher capacitance loss of the PANI electrode should be resulted from the volumetric changes due to the insertion/release of ions, during the long-term charge/discharge cycling.[5-7] While the CPANI electrode had a high retention of 65 % of its initial capacitance after 1300 cycles, indicating a long-term electrochemical stability. In comparison with the PANI electrode, the enhanced electrochemical stability of the CPANI electrode might be mainly caused by the crosslinked structure, which significantly enhance the mechanical property and efficiently hindered the deformation of the conductive polymer during the long charge/discharge process.

4. CONCLUSIONS

In summary, the crosslinked polyaniline nanorods (CPANI), synthesized by chemical oxidative polymerization of aniline in present of *p*-phenylenediamine and triphenylamine as crosslinkers with ammonium persulfate as oxidant, was investigated as the electrode material for supercapacitor for the first time. The CPANI showed regular and order nano-fibrous morphology. The electrical conductivity of the CPANI nanorods was almost 8 times higher than the PANI, reached 33.3 S cm^{-1}. The specific capacitance of the CPANI electrode was 455.1 F g^{-1} at the scan rate of 1 mV s^{-1}, much higher than 286.7 F g^{-1} of the PANI electrode. Moreover, the retention ratio of specific capacitance of the CPANI is much higher than the PANI electrode. The results

demonstrated that the crosslinking polymerization could be used as a promising approach to improve the electrochemical performance of the conducting polymer electrodes.

ACKNOWLEDGMENTS

This work was supported by the Natural Science Foundation of Gansu Province (Grant No. 1107RJZA213) and the Fundamental Research Funds for the Central Universities (Grant No. lzujbky-2011-21 and lzujbky-2013-237).

REFERENCES

(1) B. E. Conway, Electrochemical Supercapacitors: Scientific Fundamentals and Technological Applications, Plenum, New York, 1999.

(2) C. C. Hu, K. H. Chang, M. C. Lin and Y. T. Wu, *Nano Lett.*, 2006, 6, 2690.

(3) G. Gryglewicz, J. Machnikowski, E. L. Grabowska, G. Lota and E. Frackowiak, *Electrochem. Acta*, 2005, 50, 1197.

(4) G. Ciric-Marjanovic, *Synth. Met.*, 2013, 177, 1.

(5) X. W. Li, H. Zhang, G. C. Wang and Z. H. Jiang, *J. Mater. Chem.*, 2010, 20, 10598.

(6) J. H. Park, O. O. Park, K. H. Shin, C. S. Jin and J. H. Kim, *Electrochem. Solid State Lett.*, 2002, 5, H7.

(7) I. Kovalenko, D. G. Bucknall and G. Yushin, *Adv. Funct. Mater.*, 2010, 20, 3979.

(8) J. G. Wang, Y. Yang, Z. H. Huang and F. Y. Kang, *J. Power Sources*, 2012, 204, 236.

(9) X. Li, W. P. Gan, F. Zheng, L. L. Li, N. N. Zhu and X. Q. Huang, *Synth. Met.*, 2012, 162, 953.

(10) S. A. Iranagh, L. Eskandarian and R. Mohammadi, *Synth. Met.*, 2013, 172, 49.

(11) K. Zhang, L. L. Zhang, X. S. Zhao and J. S. Wu, *Chem. Mater.*, 2010, 22, 1392.

(12) Y.-C. Lin, F.-H. Hsu and T.-M. Wu, *Synth. Met.*, 2013, 184, 29.

(13) J. Yan, T. Wei, B. Shao, Z. J. Fan, W. Z. Qian, M. L. Zhang and F. Wei, *Carbon*, 2010, 48, 487.

(14) Q. Wu, Y. X. Xu, Z. Y. Yao, A. R. Liu and G. Q. Shi, *ACS Nano*, 2010, 4, 1963.

(15) H. L. Wang, Q. L. Hao, X. J. Yang, L. D. Lu and X. A. Wang, *Nanoscale*, 2010, 2, 2164.

(16) Y. H. Jin, S. Huang, M. Zhang and M. Q. Jia, *Synth. Met.*, 2013, 168, 58.

(17) Z. H. Luo, L. H. Zhu, Y. F. Huang and H. Q. Tang, *Synth. Met.*, 2013, 175, 88.

(18) L. Li, A. R. O. Raji, H. L. Fei, Y. Yang, E. L. G. Samuel and J. M. Tour, *ACS Appl. Mater. Interfaces*, 2013, 5, 6622.

(19) J. Zhang, L. B. Kong, B. Wang, Y. C. Luo and L. Kang, *Synth. Met.*, 2009, 159, 260.

(20) Y. Zhou, Z. Y. Qin, L. Li, Y. Zhang, Y. L. Wei, L. F. Wang and M. F. Zhu, *Electrochim. Acta*, 2010, 55, 3904.

(21) S. B. Yoon, E. H. Yoon and K. B. Kim, *J. Power Sources*, 2011, 196, 10791.

(22) Z. Z. Zhu, G. C. Wang, M. Q. Sun, X. W. Li and C. Z. Li, *Electrochim. Acta*, 2011, 56, 1366.

(23) M. M. Yang, B. Cheng, H. H. Song and X. H. Chen, *Electrochim. Acta*, 2010, 55, 7021.

(24) C. Z. Meng, C. H. Liu, L. Z. Chen, C. H. Hu and S. S. Fan, *Nano Lett.*, 2010, 10, 4025.

(25) Y. Y. Yang, S. Z. Chen and L. Xu, *Macromol. Rapid Commun.*, 2011, 32, 593.

(26) J. G. Tu, J. G. Hou, W. Wang, S. Q. Jiao and H. M. Zhu, *Synth. Met.*, 2011, 161, 1255.

(27) J. C. Chiang, and A. G. MacDiarmid, *Synth. Met.*, 1986, 13, 193.

(28) Z. Ping, *J. Chem. Soc. Faraday Trans.*, 1996, 92, 3063.

(29) Y. Furukawa, T. Hara, Y. Hyodo and I. Harada, *Synth. Met.*, 1986, 16, 189.

(30) Y. Wang, H. D. Tran, L. Liao, X. F. Duan and R. B. Kaner, *J. Am. Chem. Soc.*, 2010, 132, 10365.

(31) M. X. Wan, *J. Polym. Sci.: Part A. Polym. Chem.*, 1992, 30, 543.

(32) J. Laska, M. Trznadel and A. Pron, *Mater. Sci. Forum*, 1993, 122, 177.

(33) Y. Xia, J. M. Wiesinger, A. G. MacDiarmid and A. J. Epstein, *Chem. Mater.*, 1995, 7, 443.

(34) W. S. Yin and E. Ruckenstein, *Macromolecules*, 2000, 33, 1129.

(35) T. Lindfors, C. Kvarnstrom and A. Ivaska, *J. Electroanal. Chem.*, 2002, 518, 131.

(36) P. Liu, *Synth. Met.*, 2009, 159, 148.

(37) H. K. Chaudhari and D. S. Kelkar, *Polym. Int.*, 1997, 42, 380.

(38) M. E. Jozefowicz, A. J. Epstein, J. P. Pouget, J. G. Masters, A. Ray and A. G. MacDiarmid, *Macromolecules*, 1991, 24, 5863.

(39) S. Bhadra and D. Khastgir, *Polym. Test.*, 2008, 27, 851.

(40) M. A. Shenashen, M. M. Ayad, N. Salahuddin and M. A. Youssif, *React. Funct. Polym.*, 2010, 70, 843.

(41) H. J. Niu, P. H. Luo, M. L. Zhang, L. Zhang, L. N. Hao, J. Luo, X. D. Bai and W. Wang, *Eur. Polym. J.*, 2009, 45, 3058.

(42) P. Liu, P. Zhang, D. L. Cao, L. H. Gan and Y. F. Li, *J. Mol. Struct.*, 2013, 1050, 151.

(43) A. H. Gemeay, R. G. El-Sharkawy, I. A. Mansour and A. B. Zaki, *J. Colloid Interface Sci.*, 2007, 308, 385.

(44) A. Madhankumar and N. A. Rajendran, *Synth. Met.*, 2012, 162, 176.

(45) Y. E. Miao, W. Fan, D. Chen and T. X. Liu, *ACS Appl. Mater. Interfaces*, 2013, 5, 4423.

(46) Z. Gao, W. L. Yang, J. Wang, B. Wang, Z. S. Li, Q. Liu, M. L. Zhang and L. H. Liu, *Energy Fuels*, 2013, 27, 568.

(47) Z. F. Li, H. Y. Zhang, Q. Liu, L. L. Sun, L. Stanciu and J. Xie, *ACS Appl. Mater. Interfaces*, 2013, 5, 2685.

(48) H. X. Yang, T. Song, L. Liu, A. Devadoss, F. Xia, H. Han, H. Park, W. Sigmund, K. Kwon and U. Paik, *J. Phys. Chem. C*, 2013, 117, 17376.